

Laser-power-dependent Coordination and Photo-oxidation of Zinc Tetraphenylporphyrin in Alkyl Chlorides probed by Resonance Raman Spectroscopy

G. S. S. Saini, N. K. Chaudhury and A. L. Verma*

Department of Physics, North-Eastern Hill University, Shillong 793 003, India

Changes in the axial ligation and π -cation radical formation of zinc tetraphenylporphyrin (ZnTPP) in alkyl chlorides as a function of laser power have been probed by the resonance Raman technique. ZnTPP forms weakly bound pentacoordinate species in the ground state at low laser power (< 8 mW at the sample) which dissociate mainly by a thermal process into tetracoordinate, neutral ZnTPP or its π -radical cation due to electron transfer from excited ZnTPP to CCl_4 at higher laser powers. From the dependence of photo-oxidation on the concentration of electron acceptors, excitation wavelength and solvents, it is inferred that a weak triplet complex is formed between the excited ZnTPP and electron acceptor which serves as transient species and that light-induced intermolecular charge transfer from ZnTPP to CCl_4 is the primary process involved in photo-oxidation.

Metalloporphyrins in the ground or excited electronic states are known to display a variety of photochemical and photo-physical phenomena associated with the binding and release of axial ligands. The catalytic and biological functions of haem proteins and metalloporphyrins are determined, to a large extent, by the coordination structure of the central metal and a lot of work has been reported^{1–5} on the coordination chemistry of iron porphyrins, magnesium chlorins and other metalloporphyrins. The resonance Raman (RR) technique is well established as a sensitive probe for characterizing the spin, oxidation and coordination states as well as the core size of metalloporphyrins.^{6,7} Time-resolved Raman spectroscopy^{8,9} has been employed to study the binding and release of axial ligands on the picosecond and nanosecond time domain which are mediated by excited electronic states. Raman spectroscopists often use alkyl chlorides as solvents for Raman studies of metalloporphyrins, which may form very weak axially ligated complexes. During our RR studies on ZnTPP in different alkyl chlorides, we have found power-dependent changes in axial ligation and photo-oxidation of ZnTPP which may have significant bearing on the proper interpretation of the coordination structure of metalloporphyrins in terms of Raman marker bands. Some salient aspects of our RR studies of ZnTPP in alkyl chloride solutions are reported in this paper.

Experimental

Free-base tetraphenylporphyrin (H_2TPP) was purchased from Sigma, USA. Zinc metal was inserted according to the standard procedure,¹⁰ and the product was purified by column chromatography. The purity of the sample was checked by UV-VIS spectroscopy. Spectroscopic-grade C_6H_6 , CH_2Cl_2 , CCl_4 , 1,1,2,2-tetrachloroethane, C_2Cl_4 , CS_2 and methanol were obtained from SISCO and from S.D. Chemicals, dried over CaH_2 and finally distilled prior to use. Raman spectra were recorded with a SPEX Ramalog 1403 double monochromator equipped with a cooled RCA 31034A photomultiplier and photon-counting detection system. Excitation lines were provided by Liconix 4240 HeCd and Spectra-Physics 165-09 argon-ion lasers. The spectra at low temperatures were recorded with an Air Products closed-cycle helium cryocooler working up to 10 K. The position of Raman peaks was calibrated with indene or the known bands of the solvents used. Samples were degassed using freeze-thaw cycles.

Results and Discussion

The absorption spectra of ZnTPP in well known non-coordinating solvents C_6H_6 and CH_2Cl_2 (Fig. 1) are similar and match the previously reported spectrum of ZnTPP in C_6H_6 .¹¹ With CCl_4 as a solvent, there is no detectable shift in the position of the absorption bands of ZnTPP compared to CH_2Cl_2 or C_6H_6 solutions but the R value, the ratio of the molar absorption coefficients for the Q_{01} (β) and Q_{00} (α) (*i.e.* $\epsilon_{Q_{01}}/\epsilon_{Q_{00}}$) bands, decreases slightly from 5.7 to 5.0 (Fig. 1). This is indicative of the formation of a weak complex between ZnTPP and CCl_4 in the ground state. The absorption spectra of ZnTPP in CCl_4 after irradiation with 35 mW

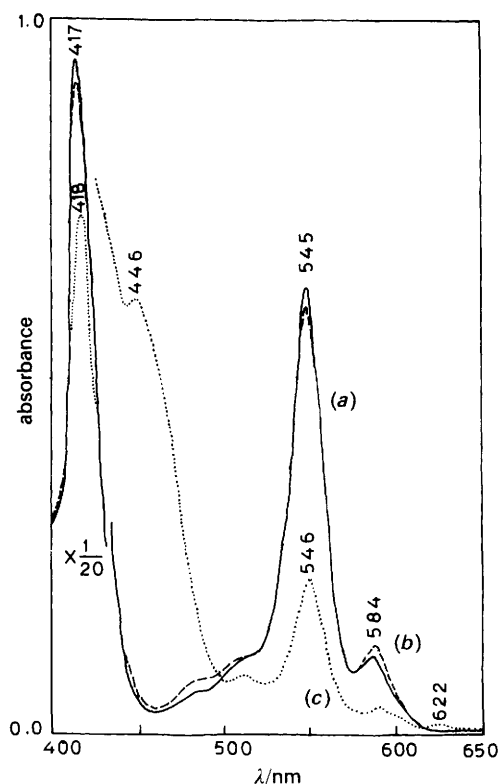


Fig. 1 Absorption spectra of ZnTPP ($\text{ca. } 3 \times 10^{-5}$ mol dm^{-3}); (a) in C_6H_6 , (b) in CCl_4 before laser excitation and (c) in CCl_4 after irradiation with 35 mW laser power at 441.6 nm under anaerobic conditions; cell pathlength 1 cm

laser power at 441.6 nm under anaerobic conditions is shown in Fig. 1(c), which agrees well with the previously reported absorption spectra of $\text{ZnTPP}^{\cdot+}$ π -radical cation.¹²

ZnTPP at Low Laser Powers (<8 mW)

The RR spectra of ZnTPP (0.5 mmol dm^{-3}) in different solvents under anaerobic conditions with 441.6 nm excitation are shown in Fig. 2. The RR spectrum in C_6H_6 shown in Fig. 2(a) is identical to the previously reported RR spectrum of tetracoordinate ZnTPP ($^4\text{ZnTPP}$) in CS_2 ¹³ and CH_2Cl_2 .¹⁴ When the laser power at the sample is kept below 8 mW for a static sample or even when *ca.* 10 mW power is used with a spinning sample, the RR spectrum in CCl_4 solution [Fig. 2(b)] shows extra features that are not present in the spectrum of $^4\text{ZnTPP}$. The ν_2 and ν_4 modes appear as doublets at 1550/1547 and 1356/1351 cm^{-1} , while the ν_{11} mode shifts from 1494 to 1490 cm^{-1} . The RR spectra of ZnTPP in some known coordinating solvents such as alcohols, tetrahydrofuran and pyridine [Fig. 2(c)] show Raman bands at

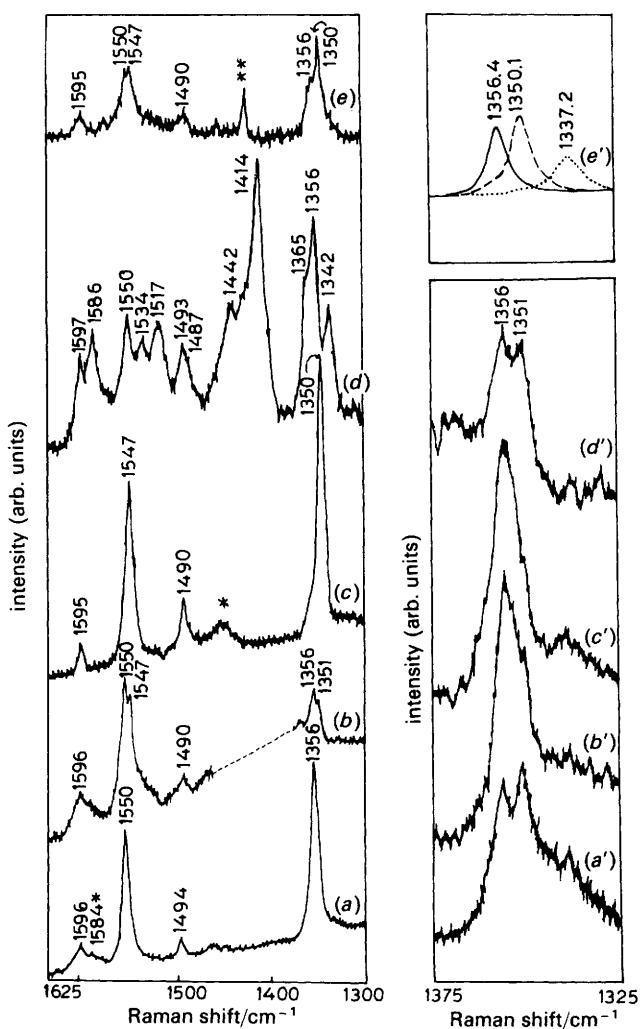


Fig. 2 RR spectra of ZnTPP (*ca.* 0.5 mmol dm^{-3}); (a) in C_6H_6 , (b) in CCl_4 at 10 mW using a rotating cell, (c) in tetrahydrofuran, (d) in CCl_4 at 35 mW and (e) in CCl_4 at around 100 K with 8 mW laser power. The right-hand side shows power-dependent changes in the relative intensity of the two components in the ν_4 region in the RR spectra of the ZnTPP in CCl_4 : (a') 2 mW; (b') 5 mW; (c') 8 mW with a static cell; (d') 8 mW with a spinning cell. The deconvoluted spectrum of (a) is shown in (e'). For all the cases, the excitation wavelength was 441.6 nm; scan speed $15 \text{ cm}^{-1} \text{ min}^{-1}$ and laser power 35 mW otherwise stated. The single and double asterisks indicate solvent bands and plasma lines, respectively

the position of the lower-wavenumber components of these doublets and ν_{11} at 1490 cm^{-1} . When the laser power at the sample in a static cell is increased to around 35 mW, the Raman signals at 1547, 1490 and 1351 cm^{-1} disappear while an entirely different spectral pattern emerges,¹⁵ as shown in Fig. 2(d). Similar RR spectra for ZnTPP in other alkyl chlorides such as $\text{CHCl}_2\text{CHCl}_2$ and C_2Cl_4 were also obtained with different laser powers as with CCl_4 solution.

The extra features at lower wavenumbers and the downward shift of the ν_{11} mode in the RR spectra of ZnTPP in alkyl chlorides at lower laser powers (<8 mW at the sample) may originate from the following sources: (i) formation of ZnTPP in the excited electronic states with long lifetimes; (ii) species produced from photo-oxidation of ZnTPP or photo-chlorination of CCl_4 ; (iii) vibrational coupling between the modes of solvent and solute molecules; (iv) changes in the relative permittivity of the solvents; or (v) formation of penta-coordinate species of ZnTPP with alkyl chlorides.

Laser excitation in the Soret or Q-band regions of ZnTPP in toluene at 300 K populates the lowest-energy excited singlet state S_1 (lifetime 2 ns) with fluorescence quantum yield $\phi = 0.04$ which populates the lowest triplet excited state T_1 by efficient intersystem crossing with $\phi = 0.88$ (lifetime 2 ms).^{15,16} The RR spectrum of ZnTPP in the excited triplet state^{13,17} is different from the RR spectra shown in Fig. 2. In particular, $^3\text{ZnTPP}$ has characteristic RR features at 1508, 1493, 1445 and 1287 cm^{-1} (with an unidentified ν_4 mode),¹⁷ but these features are absent from the spectra in Fig. 2(a)–(c). Moreover, the yield of excited ZnTPP in the triplet or singlet excited states in the steady state is expected to increase with increasing laser power, contrary to our observations from the power-dependent spectra in the ν_4 region shown in Fig. 2(a)–(c). Owing to the very short lifetime and low quantum yield, no significant population in the singlet excited state is expected with such low laser powers. Therefore the additional spectral features at lower laser power (<10 mW) cannot be associated with the excited ZnTPP in the triplet or singlet states.

Since we have used degassed solutions in our measurements, the possibility of photo-oxidation of ZnTPP is very rare. However, the irradiation of ZnTPP solution in CCl_4 with radiation within Soret band under aerobic conditions produces strong fluorescence, indicating the photoaddition of oxygen to ZnTPP to produce a fluorescent species. As no change was observed in the absorption spectrum of ZnTPP after irradiation of a degassed solution with <10 mW laser power and no bands were found at 1541, 1438, 1346 and 1297 cm^{-1} characteristic of zinc tetraphenyl phlorin,¹⁷ the extra features observed at 1351, 1547 and 1490 cm^{-1} cannot be ascribed to photoproducts of ZnTPP. Moreover, photo-chlorination from CCl_4 is expected only at higher laser powers, and as the spectral pattern did not change with varying concentrations of CCl_4 in CS_2 (an inert solvent) at lower laser powers, we can rule out this possibility also as a likely source for the extra features.

If these additional features are due to vibrational coupling between the modes of ZnTPP and CCl_4 then one would not expect these features to appear at the same position in other solvents such as $\text{CHCl}_2\text{CHCl}_2$ and C_2Cl_4 which have very distinct vibrational modes. Therefore, these extra features cannot be associated with vibrational coupling and joint excitation of the solvent and solute molecules.

The relative permittivities of C_6H_6 , CS_2 and CCl_4 are 2.27, 2.64 and 2.23.¹⁸ As they are very similar, one would expect to observe similar Raman spectra in all these solvents. On the contrary, the RR spectra in CS_2 and C_6H_6 are identical but they differ considerably from the spectra in CCl_4 [Fig. 2(a) and (b)]. Therefore the extra features observed in CCl_4 and

other alkyl chlorides cannot be explained by changes in the relative permittivity of the solvents.

In order to check the laser-power-dependent changes on the RR spectra of ZnTPP in different solvents, we found that the RR spectral pattern in CS₂, C₆H₆, CH₂Cl₂, CH₃OH and THF remains unaffected while it changes in CCl₄, CHCl₂CHCl₂ and C₂Cl₄ with laser power. The power-dependent RR spectra of ZnTPP in CCl₄ are shown in Fig. 2(a)–(c) in the ν_4 mode region where the intensity of the 1356 cm⁻¹ component increases while that of the 1550 cm⁻¹ component decreases with increasing laser power from 2 to 8 mW. When the laser power at the sample is increased beyond 10 mW in a static cell, an entirely different spectral pattern due to ⁴ZnTPP and its π -radical cation (ZnTPP^{•+}) is observed [Fig. 2(d)]. This is discussed in the next section. These observations led us to believe that ZnTPP in solvents like CCl₄, C₂Cl₂ and CHCl₂CHCl₂ forms a weak complex in the ground state which is responsible for extra Raman features at lower laser powers.

The RR spectra of ZnTPP in alcohols, tetrahydrofuran and pyridine *etc.*, which are known to coordinate at the axial position of Zn to give pentacoordinate ZnTPP (⁵ZnTPP)¹⁹ show Raman bands at the position of the low wavenumber components of these doublets at 1351 and 1547 cm⁻¹ and the ν_{11} mode at 1490 cm⁻¹. Earlier studies by Berzin⁴ also indicated that CCl₄ molecules are bound weakly at the axial positions of zinc metal.

From the shift in wavenumber of some ligation-sensitive ν_{11} , ν_4 and ν_2 modes of ZnTPP and comparison with the wavenumber of known pentacoordinated species of ZnTPP, it is clear that ZnTPP in CCl₄ and other alkyl chlorides forms a weak complex and adopts a pentacoordinate structure which also remains stable at low laser powers. When the laser power is increased, the local temperature of the sample increases, dissociating the weak pentacoordinate complex to give ⁴ZnTPP and its π -radical cation (ZnTPP^{•+}), as shown in Fig. 2(d). This point is further substantiated by our low-temperature studies where we have observed a higher concentration of ⁵ZnTPP [Fig. 2(e)]. Moreover, the pentacoordinate ZnTPP assumes a square-pyramidal structure with a concomitant increase in the core size of the macrocycle and reduction in its symmetry. This would shift the skeletal modes ν_2 , ν_{11} and ν_4 to lower wavenumber,^{20,21} as is observed in this study. In principle, one should observe a new band corresponding to a metal–ligand (Zn–CCl₄) stretching mode. This stretching mode is expected to be enhanced by excitation in the charge-transfer region which is as yet unidentified in this system.

It is known that a porphyrin can act either as an electron acceptor or donor depending on the environment, whereas CCl₄ has a slight electron-donating tendency and thus can be oxidised by electron acceptors. These properties of ZnTPP and CCl₄ may be responsible for the decrease in the ratio of the β and α band intensities (*R* value) in the absorption spectrum²² due to partial transfer of charge from the axial ligand to the porphyrin ring *via* the zinc atom. All the metal orbitals in zinc are occupied and π -type coordination involving these orbitals is not possible. However, weak ligation of CCl₄ to ZnTPP may be possible *via*: (i) interaction between the d^2sp^3 orbitals of the metal and the axial ligand giving weak σ -bonding⁴ or, (ii) the electrostatic interaction between CCl₄^{δ+} and ZnTPP^{δ-} due to partial charge transfer from CCl₄ to the porphyrin ring *via* the Zn atom in the ground state; or (iii) the ion-multipole interactions between Zn²⁺ and CCl₄ having high polarizability. All these factors may be responsible for the weak axial ligation of CCl₄ with ZnTPP. Complexation in other alkyl chlorides (CHCl₂CHCl₂, C₂Cl₄) can also be understood along similar lines.

ZnTPP at Higher Laser Powers (35–100 mW)

When the laser power at the static sample of ZnTPP in CCl₄ under anaerobic conditions was increased beyond 10 mW, we observed a different spectral pattern compared to that at lower laser power (Fig. 3). The major RR spectral features after excitation by 441.6, 457.9 and 476.5 nm radiation (*ca.* 80 mW power for the last two) can be correlated with the π -radical cation of ZnTPP (ZnTPP^{•+}) based on a comparison with the RR spectra of electrochemically generated ZnTPP^{•+},¹⁵ chemically produced ZnTPP^{•+} and characteristic electronic absorption spectra shown in Fig. 1(c). Therefore we conclude that ZnTPP in CCl₄ is photo-oxidized by irradiation with higher laser power, giving the π -radical cation (ZnTPP^{•+}) due to electron transfer from the excited ZnTPP to CCl₄. The wavenumber shift and assignment²³ of different modes on π -radical cation formation are given in Table 1. Note that the yield of photo-oxidized ZnTPP varies with the excitation wavelength, being greatest with 457.9 nm excitation and decreasing with 488.0 nm excitation, while partial demetallation is observed with 441.6 nm excitation. With 441.6 nm excitation, we observe some additional features at 1365 (ν_4), 1477 and 1542 cm⁻¹ [Fig. 3(a)] which are absent with excitation at other wavelengths. By comparison with the RR spectra of H₂TTP^{•+},²⁴ we infer that these bands originate from H₂TTP^{•+} as a result of demetallation of ZnTPP.

In an attempt to identify the transient species involved in this process, we have monitored the dependence of photo-oxidation of ZnTPP as a function of concentration of CCl₄ in CS₂ (Fig. 4) using 457.9 nm laser excitation. We have observed some extra weak features marked 'T' in Fig. 4(b) and (c) at 1508 and 1443 cm⁻¹ and a broad envelope centred around 1282 cm⁻¹ at lower concentrations of CCl₄. The

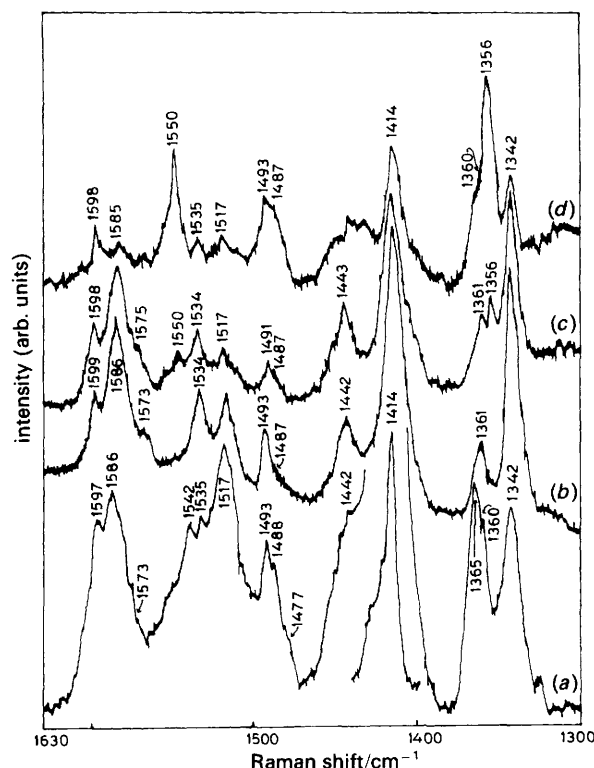


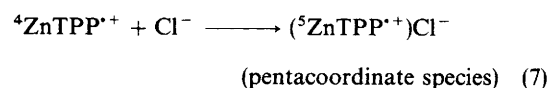
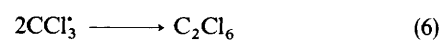
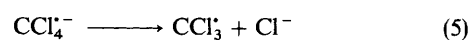
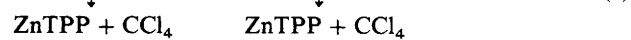
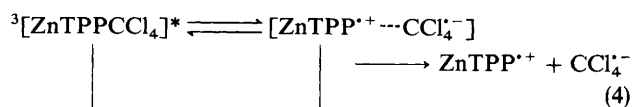
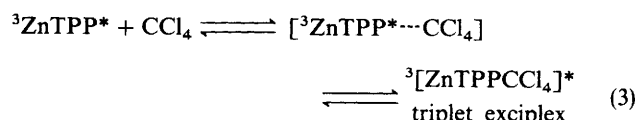
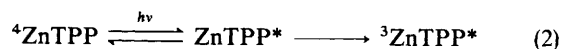
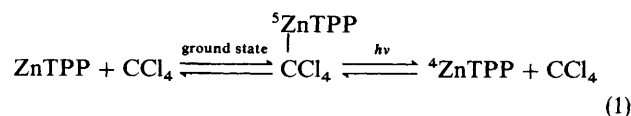
Fig. 3 RR spectra of ZnTPP (*ca.* 10⁻⁴ mol dm⁻³) in CCl₄ under anaerobic conditions with (a) 441.6, (b) 457.9, (c) 476.5 and (d) 488.0 nm excitation. Spectral conditions are similar to those in Fig. 2 except for the laser power which was 35 mW at 441.6 nm and 80 mW at other wavelengths

position of these bands is close to that observed for ZnTPP in the triplet excited state.^{13,17} During our recent studies of photo-oxidation of H₂TPP in alkyl chlorides,²⁴ we have inferred that a weak exciplex is formed between the H₂TPP in the excited triplet state and electron acceptors as a steady-state transient species during photo-oxidation of H₂TPP. From the results of Fig. 4 we suggest that an exciplex is formed between the excited triplet ZnTPP and CCl₄ as a steady-state transient species with its characteristic RR features at 1508, 1443 and 1282 cm⁻¹.

Based on different experiments and by analogy with H₂TPP,²⁴ we suggest the following mechanism for photo-oxidation of ZnTPP. The weak pentacoordinate ZnTPP-CCl₄ complex formed in the ground state dissociates into neutral molecules when it is irradiated with laser photons. The ⁴ZnTPP thus generated as well as initially present ⁴ZnTPP in solution in equilibrium is excited to the singlet state by irradiation which undergoes intersystem crossing to the triplet state, where it forms an exciplex with CCl₄. The triplet exciplex is deactivated *via* electron transfer from the macrocycle of ZnTPP to CCl₄, giving the π -radical cation of ZnTPP and the radical anion of CCl₄. CCl₄⁻ is unstable in solution and dissociates into Cl⁻ and CCl₃[·] at

room temperature. The CCl₃[·] radicals dimerize to form CCl₃CCl₃ molecule.

Schematically, the different photochemical steps may be visualized as follows:



where ZnTPP*, ³ZnTPP* and ZnTPP^{·+} represent ZnTPP in the singlet and triplet excited states and its π -radical cation, respectively. We have monitored the formation of C₂Cl₆ during photo-oxidation of ZnTPP in CCl₄ by observing directly some weak Raman features in the low-frequency region at 375 and 783 cm⁻¹ while other modes of C₂Cl₆ overlap with those of ZnTPP and ZnTPP^{·+}. The Cl⁻ ion will act as a counter-ion to stabilize the final product as the pentacoordinate ZnTPP^{·+} Cl⁻ species.

Our RR studies at low temperature (*ca.* 50 K) show that partial photo-oxidation at this temperature also takes place, indicating that long-range quantum-mechanical electron tunnelling also contributes to the electron-transfer process from ZnTPP to CCl₄, but the yield of photo-oxidation at low temperatures is very low.

Electronic and Geometric Structural Changes

From Fig. 3 and 4 and Table 1, the RR band at 1550 cm⁻¹ for neutral ZnTPP involving mainly C _{β} -C _{β} stretch with some contribution from C _{α} -C _{m} stretch (ν_2 mode) shifts downwards to 1517 cm⁻¹ on π -cation formation while some other RR bands associated with the ν_{10} [$\nu(\text{C}_\beta-\text{C}_\beta)$] and ν_4 [$\nu(\text{C}_\alpha-\text{N})$] modes also shift downwards (Table 1). Based on SCF-MO calculations,²⁵ the radicals with predominantly a_{2u} character have large spin densities located on the C _{m} and N atoms and this orbital is bonding with respect to the C _{β} -C _{β} and C _{α} -C _{m} bonds. Removal of an electron from the a_{2u} orbital on π -cation formation should weaken the C _{β} -C _{β} and C _{α} -C _{m} bonds and decrease their stretching frequencies. On the other hand, the C _{α} -N and C _{α} -C _{m} interactions are nearly non-bonding in the a_{2u} orbital and the shifts related to the modes involving these bonds are generally smaller and variable. We have observed frequency shifts of certain modes in accord with expectations for ZnTPP^{·+} radicals having predominantly a_{2u} character as observed for other tetraphenylporphyrins.^{15,24}

It is now well established that the frequencies of the high-wavenumber modes of porphyrins are correlated linearly

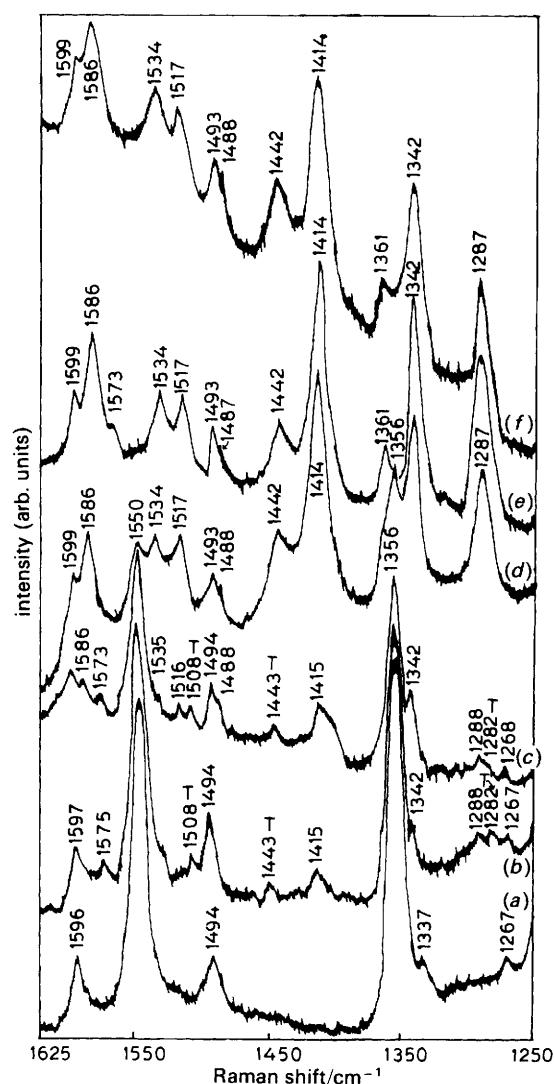


Fig. 4 RR spectra of ZnTPP with 457.9 nm excitation in (a) 100% CS₂, (b) 99.5% CS₂-0.5% CCl₄ (v/v), (c) 99% CS₂-1% CCl₄ (v/v), (d) 50% CS₂-50% CCl₄ (v/v), (e) 100% CCl₄ and (f) 98% CCl₄-2% CH₃OH (v/v). The laser power was around 80 mW and other spectral conditions are as for Fig. 2

Table 1 Resonance Raman frequencies of $^4\text{ZnTPP}$, $^5\text{ZnTPP}$ and ZnTPP^{*+}

Raman shift/cm $^{-1}$				
ZnTPP in CS $_2$ ($^4\text{ZnTPP}$)	ZnTPP in CCl $_4$ ($^5\text{ZnTPP}$ at <8 mW)	ZnTPP in CCl $_4$ (ZnTPP $^{*+}$ \geq 35 mW)	$\Delta\nu$ on π -cation formation/cm $^{-1}$	mode number and assignment ^a
1596	1596	1599	+3	ϕ_4 , $\nu(\text{C}_{\text{ph}}-\text{C}_{\text{ph}})$
1592	—	1586	-6	$\nu_{10}(\text{B}_{1g})$, $\nu(\text{C}_\alpha-\text{C}_m)_{\text{asym}}$
—	—	1573	—	$\nu_{37}(\text{E}_u)$, $\nu(\text{C}_\alpha-\text{C}_m)_{\text{asym}}$
1550	1547	1517	-33	$\nu_2(\text{A}_{1g})$, $\nu(\text{C}_\beta-\text{C}_\beta)$
—	—	1534	—	$\nu_{19}(\text{A}_{2g})$, $\nu(\text{C}_\alpha-\text{C}_m)_{\text{sym}}$
1494	1490	1493 } 1487 }	-7	$\nu_{11}(\text{B}_{1g})$, $\nu(\text{C}_\beta-\text{C}_\beta)$
—	—	1442	—	$\nu_{28}(\text{B}_{2g})$, $\nu(\text{C}_\alpha-\text{C}_m)_{\text{sym}}$
1416	—	1414	-2	$\nu_3(\text{A}_{1g})$, $\nu(\text{C}_\alpha-\text{C}_m)_{\text{sym}}$
1360	—	1361	+1	$\nu_{29}(\text{B}_{2g})$, $\nu(\text{pyrrole quarter ring})$
1356	1351	1342	-14	$\nu_4(\text{A}_{1g})$, $\nu(\text{pyrrole half ring})$
—	—	1337	—	$\nu_{20}(\text{A}_{2g})$, $\nu(\text{pyrrole quarter ring})$
—	—	1287	—	$\nu_{12}(\text{B}_{1g})$, $\nu(\text{pyrrole half ring})$
1271	—	—	—	$\nu_{27}(\text{B}_{2g})$, $\nu(\text{C}_m-\text{ph})$
1247	—	1246	-1	$\nu_{36}(\text{E}_u)$, $\nu(\text{C}_m-\text{ph})$
1235	—	1232	-3	$\nu_1(\text{A}_{1g})$, $\nu(\text{C}_m-\text{ph})$
1210	—	—	—	—
—	—	1191	—	$\nu_{34}(\text{B}_{2g})$, $\delta(\text{C}_\beta-\text{H})_{\text{asym}}$
1176	—	1180	—	—
1123	—	—	—	—
1077	—	1075	-2	$\nu_9(\text{A}_{1g})$, $\delta(\text{C}_\beta-\text{H})_{\text{sym}}$
1030	—	1033	+3	ϕ_7 , $\nu(\text{C}_{\text{ph}}-\text{C}_{\text{ph}})$
—	—	1015	—	$\nu_{22}(\text{A}_{2g})$, $\nu(\text{pyrrole half ring})_{\text{asym}}$
1004	—	1009	+5	$\nu_6(\text{A}_{1g})$, $\nu(\text{pyrrole breathing})$
995	—	993	-2	$\nu_{30}(\text{B}_{2g})$, $\nu(\text{pyrrole half ring})$

^a Mode numbering and assignment are according to ref. 23.

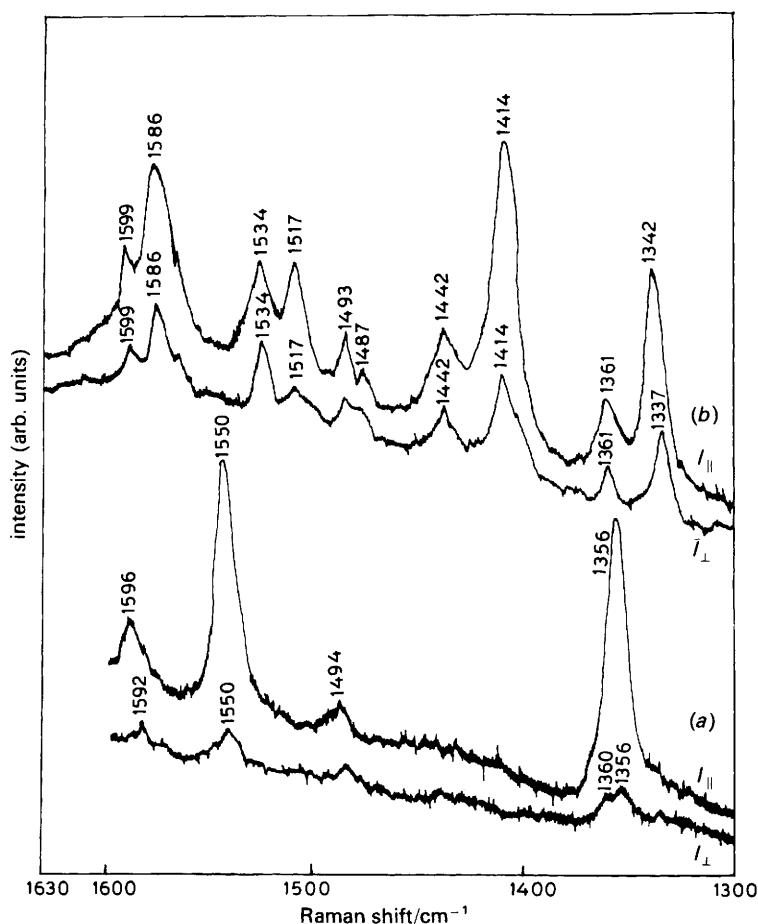


Fig. 5 Polarized RR spectra of ZnTPP (a) in CS $_2$; (b) in CCl $_4$ with 457.9 nm excitation line in parallel ($I_{||}$) and perpendicular (I_{\perp}) polarization geometries. In (a), the depolarized component at 1592 cm $^{-1}$ corresponding to the ν_{10} mode becomes clear

with the core size of the macrocycle.⁷ Therefore the shift in ν_2 from 1550 to 1517 cm^{-1} and other high-wavenumber modes (ν_{11} from 1494 to 1487 cm^{-1} and ν_4 from 1356 to 1342 cm^{-1}) may also indicate the core expansion of ZnTPP macrocycle on photo-oxidation, since axially bound Cl^- would attract the Zn metal out of the porphyrin plane. Although there are no data on the core size of $\text{ZnTPP}^{+\cdot} \text{Cl}^-$, from the X-ray analysis of $\text{ZnTPP}^{+\cdot} \text{ClO}_4^-$, Scheidt *et al.*²⁶ obtained 2.047 Å for the core size of the latter complex, which is larger than the core size of ZnTPP (2.036 Å). In π -radical cations, saddle distortion may also contribute to the core expansion.^{27,28}

Intensity Enhancement of Certain Modes

The intensities of certain modes show enhancement in the RR spectra of the π -radical cation. Almost all the modes involving $\text{C}_\alpha-\text{C}_m$ stretching, particularly the ν_3 , ν_{10} , ν_{19} and ν_{28} modes, gain intensity. The ν_{19} mode is generally not seen with excitation in the Soret region due to its A_{2g} (under D_{4h}) symmetry, but when the symmetry of the molecule is lowered from D_{4h} to D_{2d} on π -cation formation,¹⁵ the A_{2g} vibration becomes B_{1g} and can be observed as the depolarized mode as shown in Fig. 5. Therefore we associate the 1535 cm^{-1} band with ν_{19} and the 1586 cm^{-1} band with ν_{10} modes, respectively [Fig. 4(e) and 5(b)]. This assignment gains support from the previous work on $\text{Zn}^{\text{II}}\text{TMPyP}$, for which the RR band at 1530 cm^{-1} was assigned to the ν_{19} mode by Song *et al.*²⁹

Financial assistance from the Department of Science and Technology and Department of Atomic Energy, Govt. of India, is gratefully acknowledged.

References

- J. W. Buchler, *Porphyrins and Metalloporphyrins*, ed. K. M. Smith, Elsevier, Amsterdam, 1975, p. 157.
- P. Hambright, ref. 1, p. 233.
- D. Kim and T. G. Spiro, *J. Am. Chem. Soc.*, 1986, **108**, 2099.
- B. D. Berzin, *Coordination Compounds of Porphyrins and Phthalocyanines*, transl. V. G. Vopian, John Wiley, New York, 1981.
- J. J. Katz, L. L. Shipman, T. M. Cotton and T. R. Johnson, *The Porphyrins*, ed. D. Dolphin, Academic Press, New York, 1978, vol. V, p. 402.
- T. G. Spiro, *Iron Porphyrins*, ed. A. B. P. Lever and H. B. Gray, Addison-Wesley, Reading, MA, 1983, part II, p. 89.
- T. Kitagawa and Y. Ozaki, *Struct. Bonding (Berlin)*, 1987, **64**, 71.
- E. W. Findsen, J. A. Shelnut, J. M. Friedman and M. R. Ondrias, *Chem. Phys. Lett.*, 1986, **126**, 465.
- E. W. Findsen, J. A. Shelnut and M. R. Ondrias, *J. Phys. Chem.*, 1988, **92**, 307.
- J. H. Fuhrhop and K. M. Smith, ref. 1, p. 757.
- M. Gouterman, ref. 5, vol. III, p. 1.
- Z. Gasyna, W. R. Browett and M. J. Stillman, *Inorg. Chem.*, 1985, **24**, 2440.
- V. A. Walters, J. C. de Paula, G. T. Babcock and G. E. Leroi, *J. Am. Chem. Soc.*, 1989, **111**, 8300.
- H. Yamaguchi, M. Nakano and K. Itoh, *Chem. Lett.*, 1982, 1397.
- R. S. Czernuszewicz, K. A. Macor, X-Y. Li, J. R. Kincaid and T. G. Spiro, *J. Chem. Soc.*, 1989, **111**, 3860.
- A. Harriman, G. Porter and N. Searle, *J. Chem. Soc., Faraday Trans. 2*, 1979, **75**, 1515.
- R. A. Reed, R. Purello, K. Prendergast and T. G. Spiro, *J. Phys. Chem.*, 1991, **95**, 9720.
- Handbook of Organic Chemistry*, ed. J. A. Dean, McGraw-Hill, New York, 1987.
- C. K. Schauer, O. P. Anderson, S. S. Eaton and G. R. Eaton, *Inorg. Chem.*, 1985, **24**, 4082.
- J. D. Strong, T. G. Spiro, R. J. Kubaska and S. I. Shupack, *J. Raman Spectrosc.*, 1980, **9**, 312.
- D. M. Collins and J. L. Hoard, *J. Am. Chem. Soc.*, 1970, **92**, 3261.
- H. Seki, M. Hoshino and H. Shizuka, *J. Phys. Chem.*, 1989, **93**, 3630.
- X. Y. Li, R. S. Czernuszewicz, J. R. Kincaid, Y. O. Su and T. G. Spiro, *J. Phys. Chem.*, 1990, **94**, 31.
- G. S. S. Saini, N. K. Chaudhury and A. L. Verma, *Photochem. Photobiol.*, 1992, **55**, 815.
- D. Spangler, G. M. Maggiora, L. L. Shipman and R. E. Chriteferson, *J. Am. Chem. Soc.*, 1977, **99**, 7478.
- W. E. Scheidt, M. E. Kastner and K. Hatano, *Inorg. Chem.*, 1978, **17**, 706.
- G. Buisson, A. Deronzier, E. Duee, P. Gans, J. C. Marchon and J. R. Regnard, *J. Am. Chem. Soc.*, 1982, **104**, 6793.
- P. Gans, G. Buisson, E. Duee, J. C. Marchon, E. S. Erler, W. F. Scholz and C. A. Reed, *J. Am. Chem. Soc.*, 1986, **108**, 1223.
- O. K. Song, M-J. Yoon and D. Kim, *J. Raman Spectrosc.*, 1989, **20**, 739.